



INTERNATIONAL ATOMIC ENERGY AGENCY
UNITED NATIONS EDUCATIONAL, SCIENTIFIC AND CULTURAL ORGANIZATION



INTERNATIONAL CENTRE FOR THEORETICAL PHYSICS
34100 TRIESTE (ITALY) · P.O.B. 500 · MIRAMARE · STRADA COSTIERA 11 · TELEPHONE: 3240-1
CABLE: CENTRATOM · TELEX 460392-1

SMR/382- 12

WORKSHOP ON SPACE PHYSICS:
"Materials in Micogravity"
27 February - 17 March 1989

"Impurities"



E. KALDIS
ETH
Zurich, Switzerland

Please note: These are preliminary notes intended for internal distribution only.

MAIN GOAL OF THE MATERIALS RESEARCH in
conjunction with the VAPOR GROWTH OF PERFECT
CRYSTALS of $\alpha\text{-AgI}_2$



Discovery and elimination
of the sources of traps

Sources of Traps can be

- {
1 mechanical (bottom sawing) } handling!
{ 2 structural (rocking curves) } many problems solved
already

- ① DENSITY dependent Viewgraph same
② nonstoichiometry dependent
③ crystal growth dependent

1. Plastic deformation

Critical resolved shear stress (CRSS)

$$0.5 \text{ lb/sq in} = 0.003 \text{ MPa}$$

Georgeson + Milstein (1985)

$$\frac{(\gamma)}{(A)} \text{ (vit} = 5.41$$

$$d_{\text{AgI}_2} = 6.4 \text{ g/cm}^3$$

↓
crystal dimensions 2.5-3.0 cm (30 cm²)
plastic deformation under it's weight.

3. Purity

- SSMs high concentration of hydrocarbons.
- Main source iodide Viewgraph
- Where are the hydrocarbons located in the lattice?

Possible adsorption sites

van d. Waals layers
Viewgraph
Channels in the lattice
Viewgraph

In case of INTERCALATION changes of the lattice constants should become visible?

Viewgraph
No significant changes

Alternative explanation

Inhomogeneous incorporation
of impurities, breaking the
van d. Waals layers
(Mosaic Structure) Viewgraph

NICOLAU

Work supporting this: Inclusions Viewgraphs

MUHEIM et al. 1983 (ETH Zurich)

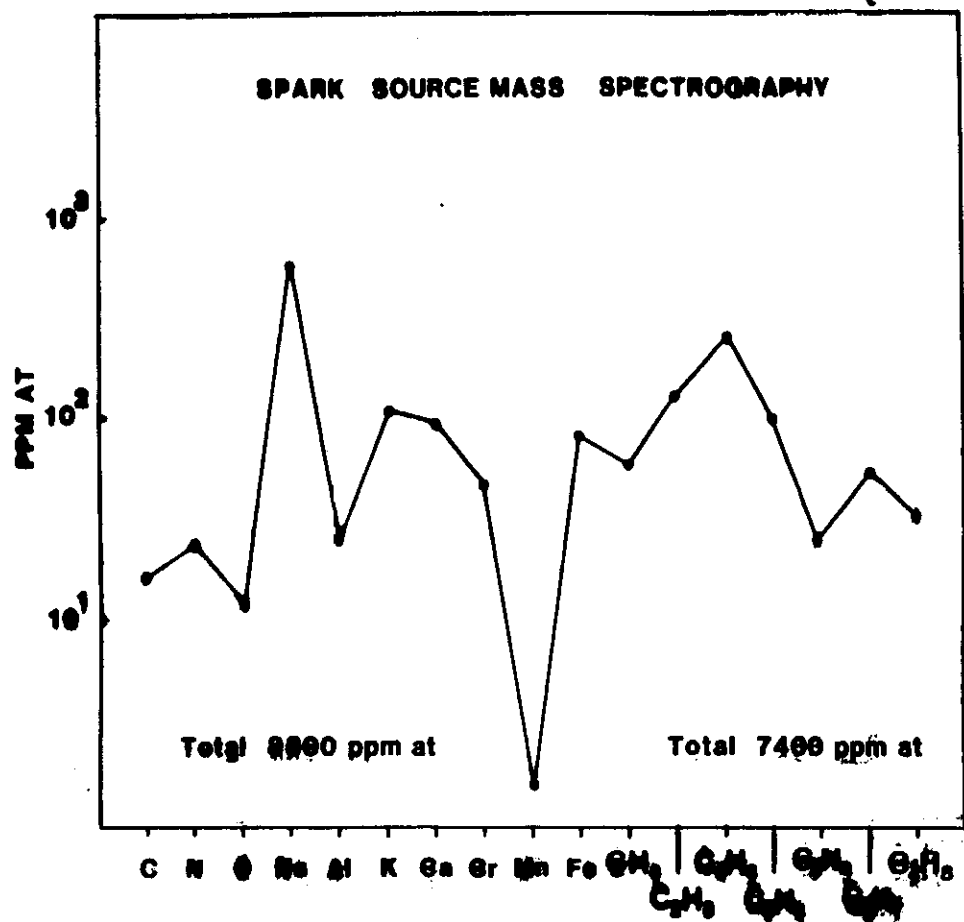
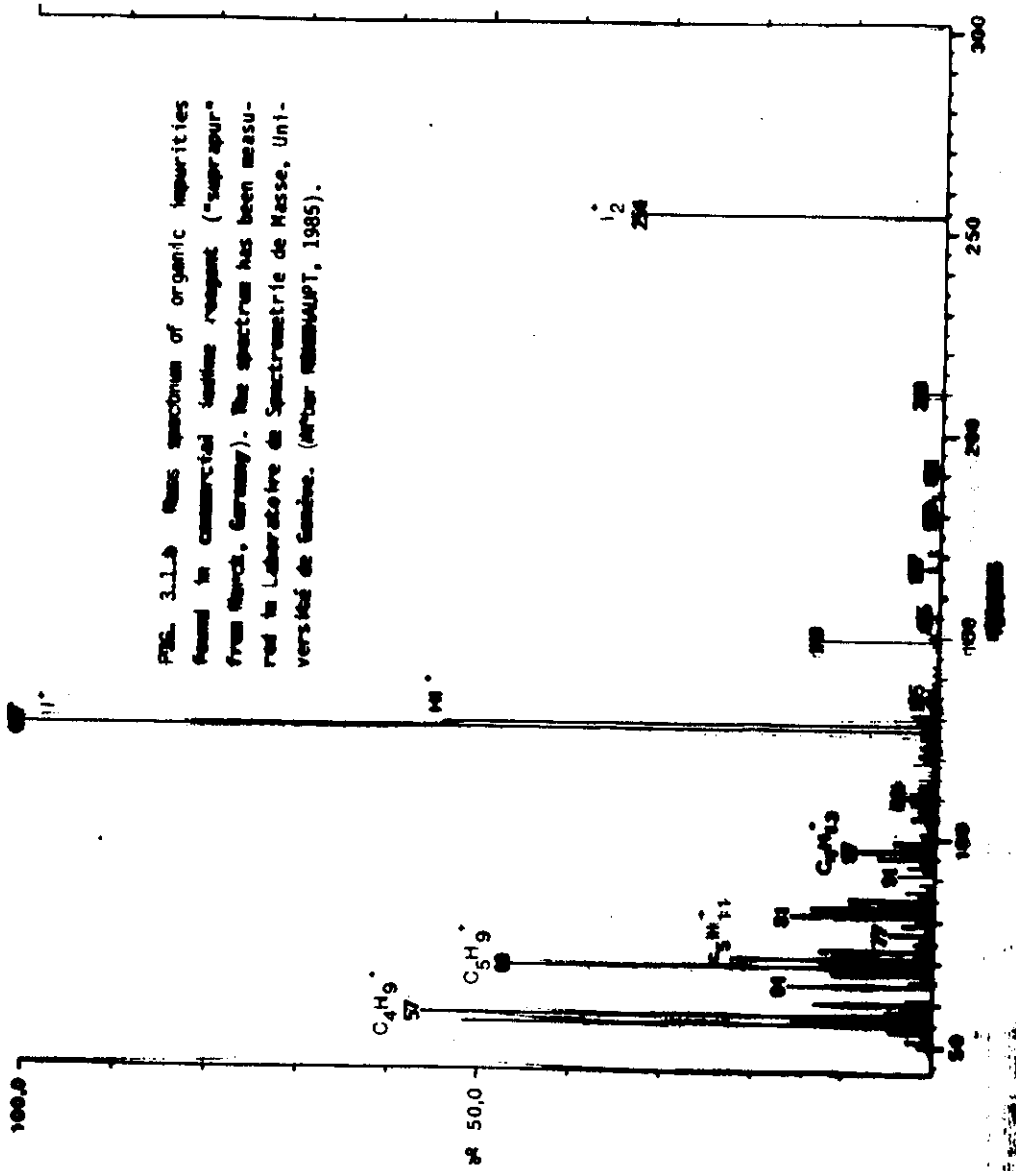


Fig. 2 Typical concentration distribution of inorganic and organic impurities in mercuric iodide as measured by SSMS.



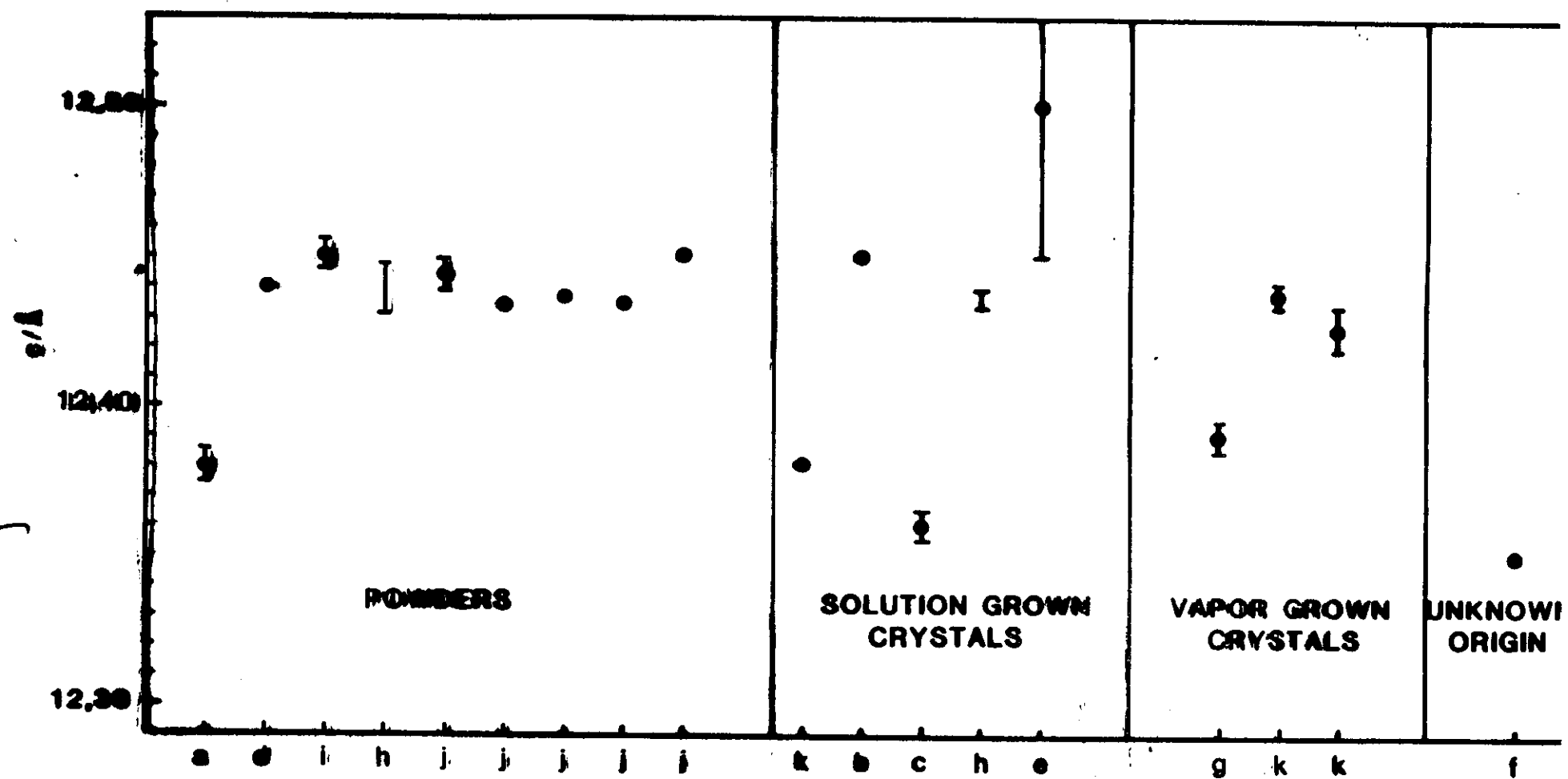


Fig. 4.5 b) Lattice constant c of the red mercuric iodide as measured since 1890 by various authors. (For references see Tab. 4.2).

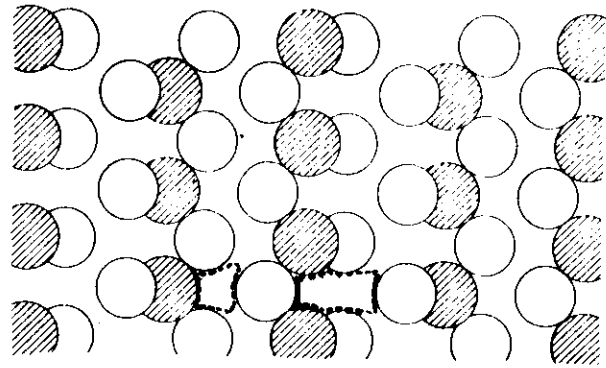


FIG. 4.6 Structure of $\alpha\text{-HgI}_2$ as seen along a -axis (only the first three layers of atoms have been shown). 100% of covalent bonding between Hg and I atoms is assumed. Note two kinds of channels

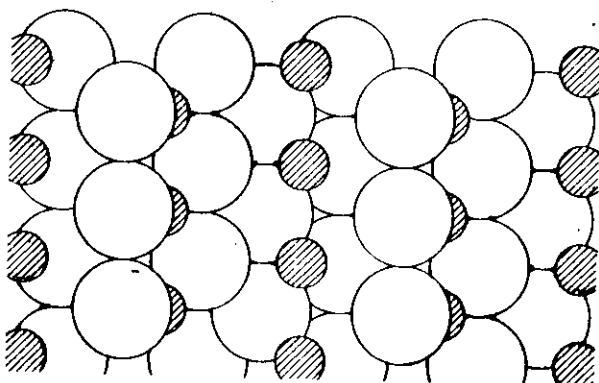


FIG. 4.7 Structure of $\alpha\text{-HgI}_2$ as seen along a -axis (only the first three layers of atoms have been shown). 100% of ionic bonding is assumed.

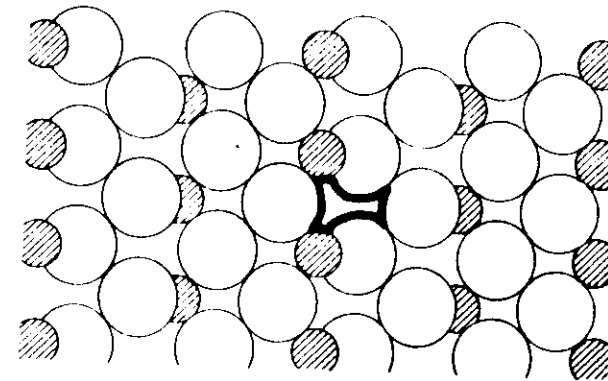
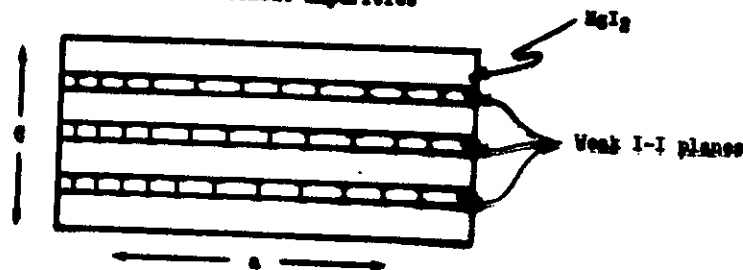


FIG. 4.8 Structure of $\alpha\text{-HgI}_2$ as seen along a -axis (only the first three layers of atoms have been shown). 30% of ionic bonding is assumed.

channels few

Huth USC 1929

a) Theoretical - without impurities



b) "Idealized" - finite but uniform impurity distribution



c) "Actual" - finite and non-uniform impurity distribution

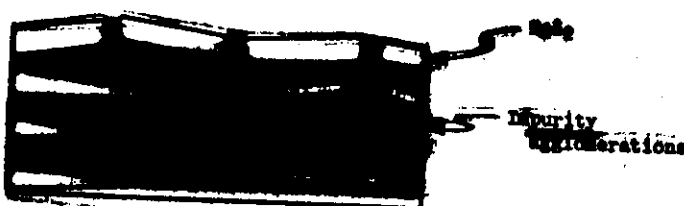


Figure 3.1

NICOLAU (Private communication)

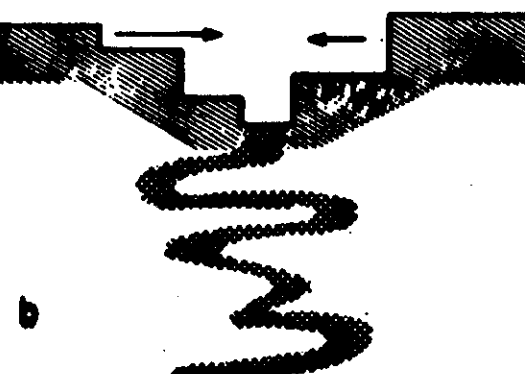
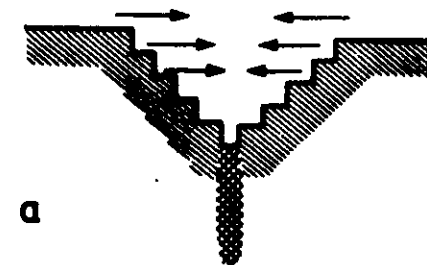


Fig. 6.13 Valleys at the growth interface, schematic cross sections. The direction of step and terrace motion is indicated by arrows. At the valley bed, where the steps meet and annihilate, dopants and impurities may be preferentially trapped or rejected. The trace of the valley may be straight as shown in (a), when the steps moving towards each other are regular. The valley trace may "oscillate" in the lateral direction as shown in (b), when the step trains are irregular. After LU and BAUSER, 1969.

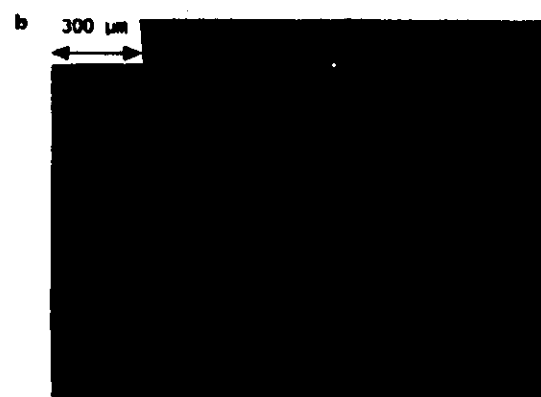
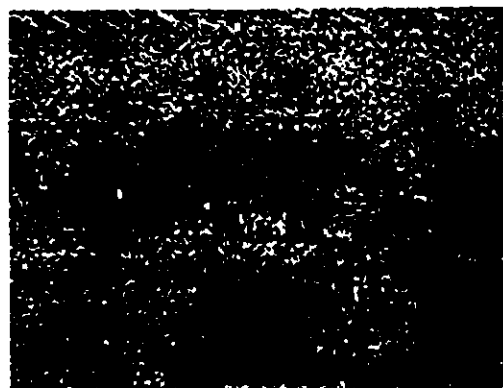


Fig.6.14 a) Straight valley traces on the as grown {110} face of a solution grown (LETI-30) α -HgI₂ crystal. Optical microscopy reflected light, x32 magnification. After NICOLAU, 1986.

b) Sinusoidal shaped arrangement of foreign particles trapped in α -HgI₂ crystal grown in a vertical furnace by TOM method. After SCHIEBER et al., 1976.

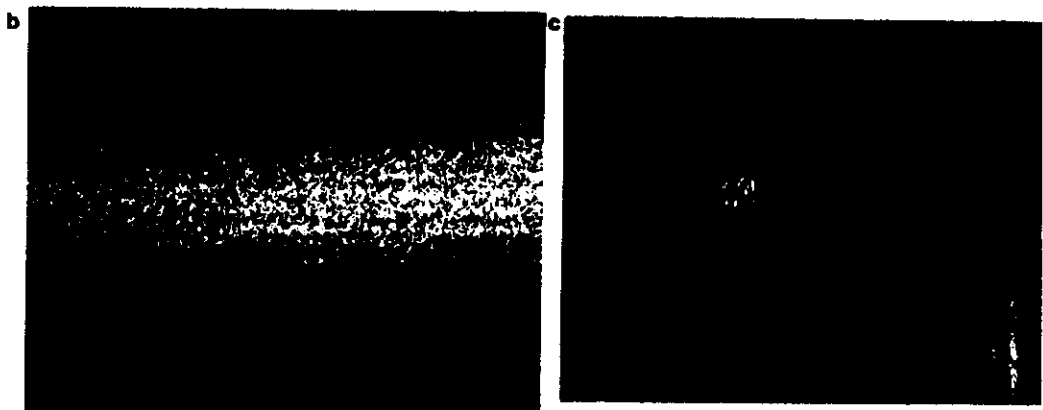


Fig.6.8 Optically clear solution grown (LETI-32) α -HgI₂ crystal (a) illuminated by a laser beam ($\lambda=608-613\mu m$) of 1mm diameter. Much more scattering of the beam is seen in the <110> (b) than in the <001> (c) direction. After NICOLAU, 1986.

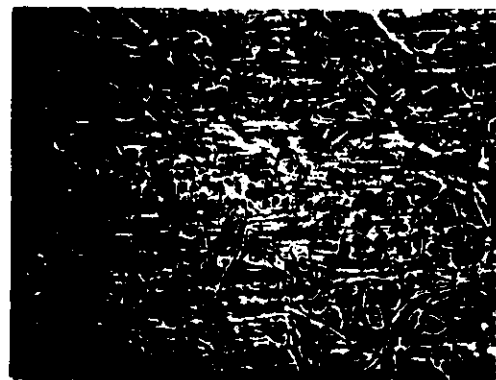


Fig. 6.15 Voids (black dots) of 10-20 μm diameter in a vapor grown (EG&G, S 6-24) α -HgI₂ crystal. Sawn and polished (110) plane optical image, x100 magnification, reflected light. After NICOLAU, 1986.

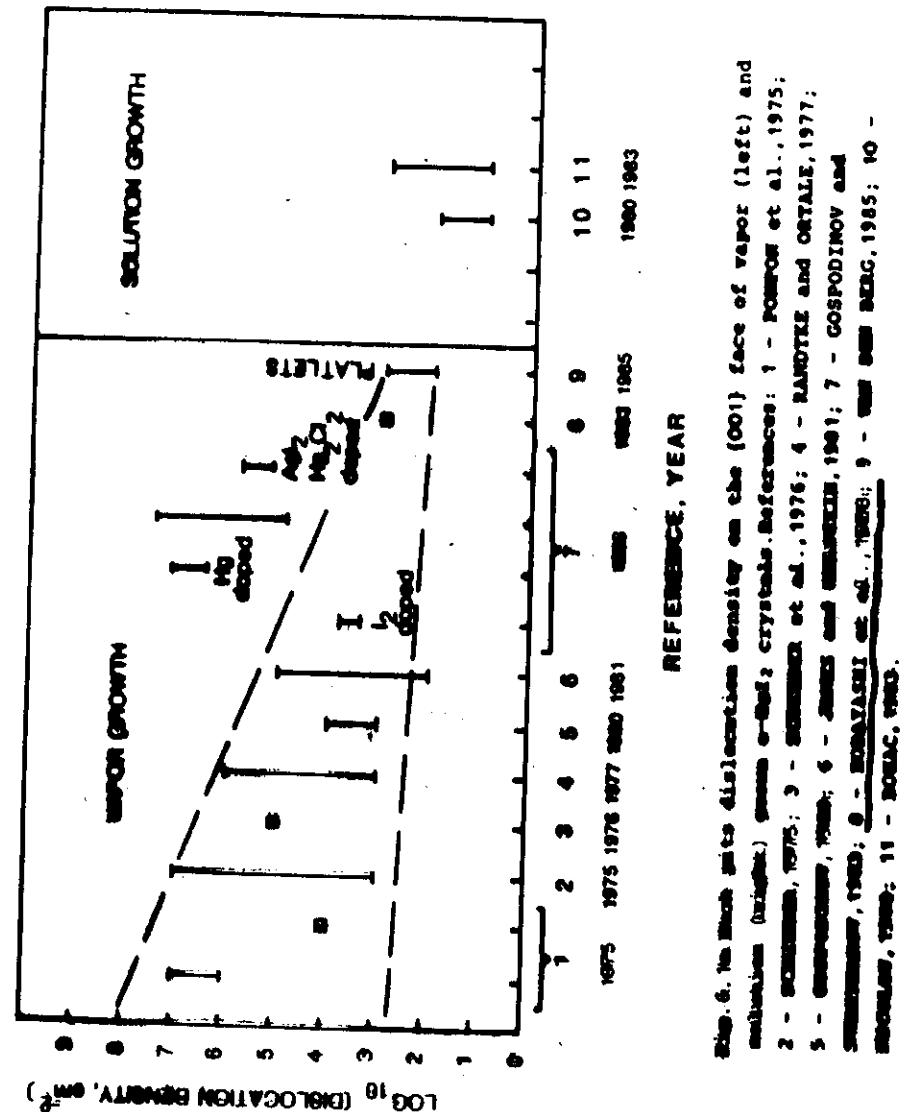


Fig. 6.16 Mean dislocation densities on the (001) face of vapor (left) and solution (right) α -HgI₂ crystals. References: 1 - PONROV et al., 1975; 2 - NICOLAU, 1975; 3 - NICOLAU et al., 1976; 4 - RANOTKE and OETALI, 1977; 5 - NICOLAU, 1977; 6 - NICOLAU and NICOLAU, 1981; 7 - GOSPODINOV and NICOLAU, 1982; 8 - ROMAGNANI et al., 1983; 9 - NICOLAU and NICOLAU, 1985; 10 - NICOLAU, 1985; 11 - NICOLAU, 1985.

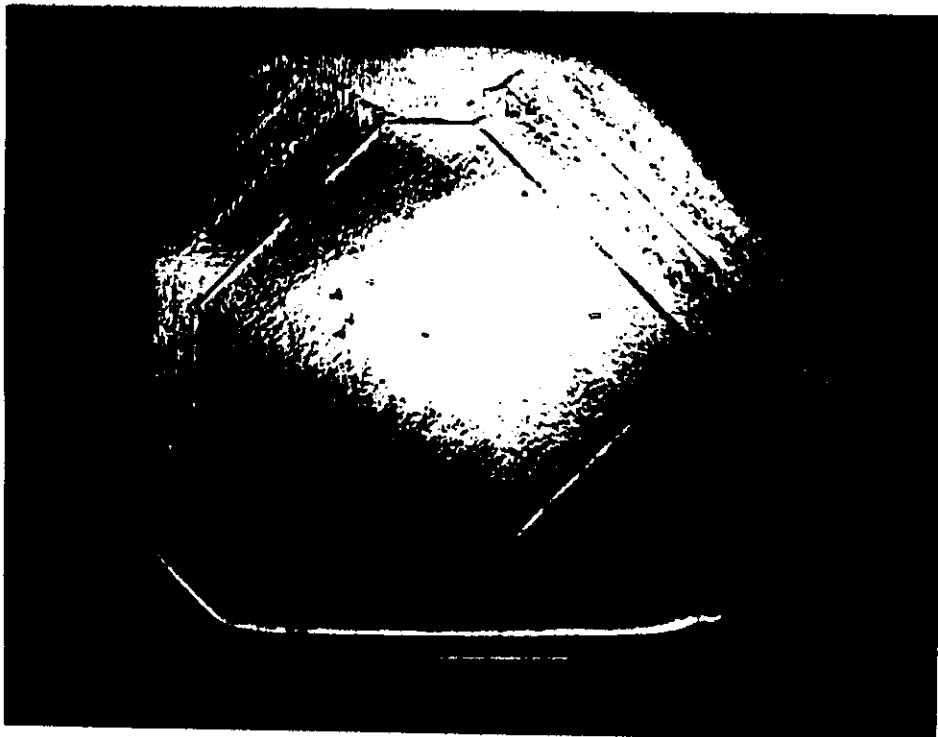


Fig.6.1d As grown crystal surface after polishing and etching. Notice the low concentration of pyramidal etch pits in the central part corresponding to a dislocation density of 10^3 cm^{-2} . Bands with high concentration of flat bottom etch pits appear at the outer parts. After KOBAYASHI et al., 1983.



Fig.6.1b SEM micrograph which shows emergence point possibly due to a dislocation. After KOBAYASHI et al., 1983.



Fig.6.1c SEM micrograph of the flat bottom etch pits found in mercuric iodide crystals by KOBAYASHI et al., 1983.

Straight forward conclusion

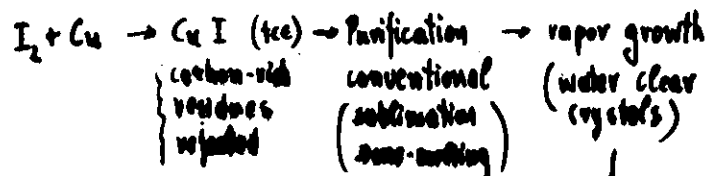
A new, nonconventional PURIFICATION METHOD

is conditio sine qua non for further
improvement of the crystal perfection:

~ (Picotka, Kaldis, 1983) «Lattice Filtering»

use UHV, oil-free system (mercury pumps, 10^{-10} torr at best)

Introduces iodine in a closed packed lattice, having no space
for hydrocarbon intercalation



↓
decomposition

↓
in situ reaction
of I_2 with $Hg \rightarrow HgI_2$

Drawback: very small scale production (100g/3 months!)

~ A much more efficient method (1kg/week) is now tested
(Picotka, Kaldis 1986)

Ampoule for crystal growth

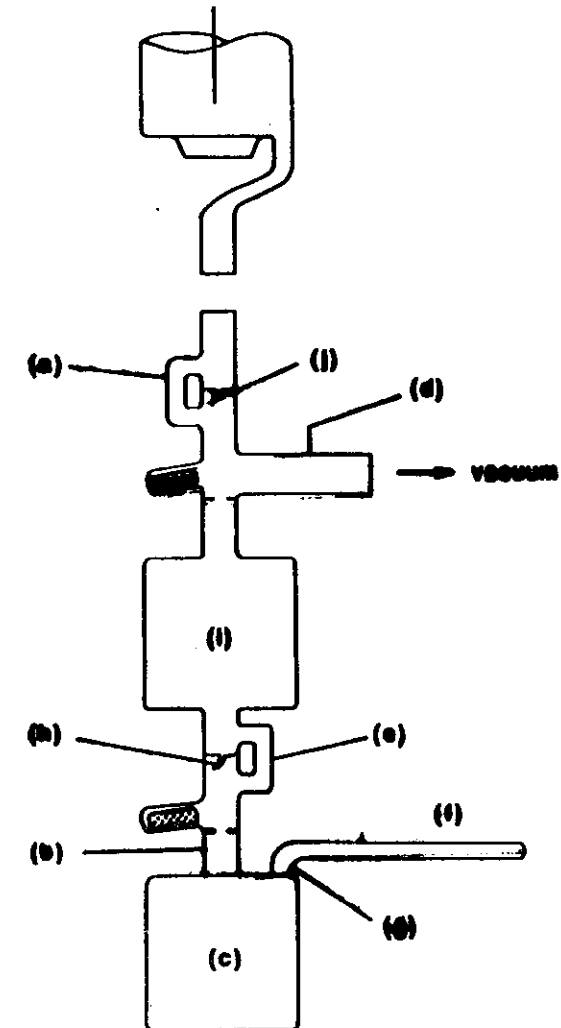


Fig. 26